Clays and Clay Minerals, Vol. 36, No. 3, 249–257, 1988.

TRANSFORMATION OF HAUSMANNITE INTO BIRNESSITE IN ALKALINE MEDIA

R. M. CORNELL[1] AND R. GIOVANOLI[2]

[1] ETH Zürich, Laboratory for Inorganic Chemistry, ETH-Zentrum
CH-8092 Zürich, Switzerland

[2] University of Bern, Laboratory for Electronmicroscopy
Freiestrasse 3, CH-3000 Bern 9, Switzerland

Abstract—The transformation of hausmannite (Mn_3O_4) into a K-bearing, 7-Å phyllomanganate (K-birnessite) in KOH was followed using X-ray powder diffraction and transmission electron microscopy. The transformation involved dissolution of Mn_3O_4 followed by reprecipitation of the 7-Å phase. The rate-determining step was the dissolution of Mn_3O_4. The reaction was accelerated by increasing the pH and/or the temperature of the system.

K-birnessite precipitated initially as thin, irregular plates and films that gradually recrystallized to thicker, more structured plates and laths. A pseudohexagonal unit cell with $a_0 = 2.87$ Å and $c_0 = 7.09$ Å was found for this phase. Synthetic K-birnessite was stable in KOH at 70°C for many months. In neutral to slightly acidic media it converted rapidly to $Mn_7O_{13} \cdot 5H_2O$, and in more acid media, it dissolved and reprecipitated as γ-MnO_2. The replacement of K^+ by Na^+ was not achieved. Jacobsite and magnetite also underwent a dissolution/reprecipitation transformation in KOH.

Key Words—Alkaline solution, Birnessite, Dissolution, Hausmannite, Manganese, Synthesis.

INTRODUCTION

The 7-Å phyllomanganates (or birnessites) are widely distributed in soils and sediments. Their reactivity makes them important regulators of Mn availability in solution and also of trace metal uptake. These compounds consist of sheets of edge-sharing $Mn(IV)O_6$ octahedra interlayered with sheets of water molecules. Systematic Mn(IV) vacancies in the sheets of $Mn(IV)O_6$ octahedra lead to an overall negative charge on the sheets. This charge is compensated for by variable amounts of Mn^{2+} and/or Mn^{3+} ions in the interlayers above and below the vacancies in the framework sheets (Giovanoli *et al.*, 1970). These birnessites usually contain other interlayer cations, most commonly Na^+, but various transition metal ions can be accommodated as well. Such a structure permits the existence of a series of birnessites having a range of structures and degrees of ordering.

Most Mn oxides can be produced by a variety of pathways, and interconversions between different oxides form an important feature of this class of compounds (Giovanoli, 1976). Although poorly crystallized birnessites can be obtained by precipitation from $KMnO_4$ solution, the commonest preparative route involves oxidation of $Mn(OH)_2$ to a 10-Å phyllomanganate (or buserite) followed by dehydration to the 7-Å phase (Giovanoli *et al.*, 1976).

This paper reports the formation of birnessite by an entirely new pathway involving dissolution of hausmannite (Mn_3O_4) in KOH. The transformation was followed by X-ray powder diffraction (XRD) and by transmission electron microscopy (TEM), and the birnessites produced were characterized. Two questions were examined; (1) are the birnessites prepared by a dissolution/reprecipitation reaction different from those obtained by topotactic transformation of $Mn(OH)_2$; and (2) do the Na- and K-birnessites have similar properties?

Ultimately this study should provide information about the mechanism by which birnessite forms in soils. In natural waters oxidation of Mn^{2+} leads to Mn_3O_4 and β-MnOOH which further transform to γ-MnOOH (Stumm and Giovanoli, 1976). Hem and Lind (1983) used thermodynamic arguments to show that in such systems disproportionation reactions can convert Mn^{3+} products to $Mn(IV)O_2$. The pathways by which birnessites form in soils have not been clearly established; it seems probable, however, that as in natural waters, a dissolution/reprecipitation mechanism is involved.

EXPERIMENTAL METHODS

The transformation experiments were carried out by reacting 0.4 g of Mn_3O_4 (or Fe_3O_4 (magnetite) or $MnFe_2O_4$ (jacobsite)) with 100 ml of KOH or NaOH. The oxide was lightly ground in an agate mortar to break up the aggregates of crystals. The concentration of alkali ranged from 0.001 M to 10 M. Most experiments were carried out with 1 M KOH. The temperature of transformation was usually 70°C, although some experiments were conducted at 25° or 90°C. Additional experiments involved transformations in twice-distilled water or in 0.1 M HNO_3. The transformations took from weeks to months to complete. The product

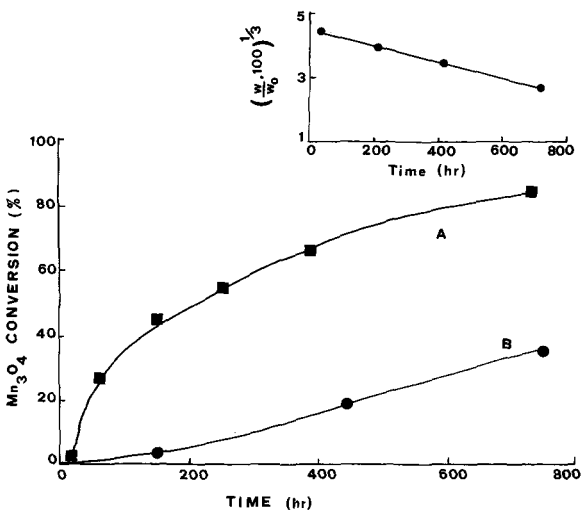

Figure 1. Extent of transformation of Mn_3O_4 vs. time: (A) 1 M KOH, (B) 0.01 M KOH, 70°C. Inset = cube root plot for the conversion in 1 M KOH.

was washed, dried at room temperature, and examined using XRD, TEM, and energy-dispersive X-ray analysis (EDX). At no stage during the experiment did atomic absorption spectroscopy (AA) detect any Mn in solution (sensitivity = 0.1 ppm Mn). The kinetics of the transformation was followed using a series of Mn_3O_4/KOH suspensions and, at predetermined intervals, removing a suspension for XRD and TEM examination.

XRD patterns were obtained using a Guinier-Enraf camera (Mk.IV) with Fe$K\alpha_1$ radiation. Preliminary experiments showed no difference in the XRD patterns whether the sample was examined as a dry powder or a wet paste; therefore in subsequent examinations a dried powder was used. The proportions of Mn_3O_4 and 7-Å phase in the product were estimated by comparing the XRD patterns of the products with those made by mixing known amounts of synthetic Mn_3O_4 and a K-birnessite. The 111 peak of Mn_3O_4 and the 00.2 peak of the 7-Å phase were used.

TEMs were obtained with a Hitachi H-600-2 (100 kV) electron microscope equipped with a Tracor TN 5400 energy-dispersive X-ray spectrometer. For TEM examination the samples were dispersed in twice-distilled water by an ultrasonic treatment, and a drop of suspension was dried on a carbon-coated bronze grid. For EDX spectra the sample was dried on a graphitized nylon grid. Selected-area electron diffraction (SAD) patterns were obtained using gold as an internal standard.

To determine the proportions of Na^+ or K^+ in the 7-Å phase 10 mg of sample was dissolved in 10 ml of 2 M HCl. Analysis for Na, K, and Mn was carried out using AA.

Mn_3O_4 was prepared by passing O_2 through a suspension formed by mixing 0.5 M $MnCl_2$ and 1 M NaOH at 60°C (Giovanoli *et al.*, 1976). The resulting Mn_3O_4 (BET surface area = 29 m^2/g) was washed and dried. A sample of commercial Fe_3O_4 (BET surface area = 1 m^2/g) was obtained from Bayer Ltd. (Krefeld, Federal Republic of Germany). Jacobsite (BET surface area = 22 m^2/g) was prepared by coprecipitating manganese(II) nitrate and ferric nitrate (Mn/(Mn + Fe) = 0.56) with 1 M KOH to pH 12 and heating the precipitate that formed at 70°C for 24 hr (Cornell and Giovanoli, 1987).

Surface areas were measured by the BET method using N_2.

RESULTS

In >0.01 M KOH or NaOH, Mn_3O_4 gradually dissolved and reprecipitated as a phyllomanganate showing characteristic XRD lines at ~7.1 and 3.5 Å. These reflections were observed for both wet and dried samples; no 10-Å phyllomanganate was noted in the product. The 7-Å phase, therefore, did not form via dehydration of a 10-Å phase, but precipitated directly from solution.

Additional experiments showed that if Mn^{2+} solutions were treated at pH 12 with KOH and held in closed vessels at 70°C, the initial poorly crystalline precipitate transformed into well-crystallized hausmannite in 24 hr. The hausmannite then slowly converted into K-birnessite.

Kinetics

In Figure 1 the extent of conversion of Mn_3O_4 into a 7-Å phase is plotted against time. The brief induction period corresponds to the time necessary to build up sufficient soluble Mn species to permit nucleation of the 7-Å phase. Following this induction period, the transformation was initially quite fast (4–5% in 24 hr). The rate of transformation decreased, however, as the reaction proceeded and the surface area of the Mn_3O_4 fell. In 1 M KOH complete conversion took about 2000 hr.

The induction period was eliminated by seeding the suspension with 5% birnessite. Seeding did not accelerate the overall transformation, however, indicating that dissolution of Mn_3O_4 was the rate-limiting step in this reaction.

Further evidence that the rate-limiting step was the reaction at the surface of the Mn_3O_4 particles comes from the observation that the bulk of the reaction can be described by the cube root law (Hixon and Crowell, 1931; Cornell *et al.*, 1975), i.e.,

$$w^{1/3} = w_0^{1/3} - kt,$$

where w_0 is the initial weight of Mn_3O_4; w is the weight of oxide after time, t; k is a constant; and t is the time of dissolution. A plot of $(w/w_0 \times 100)^{1/3}$ vs. time, shown in Figure 1 (inset), is linear for more than 80% of the reaction.

https://doi.org/10.1346/CCMN.1988.0360306 Published online by Cambridge University Press

Mn_3O_4 transformed into a 7-Å phase at OH^- concentrations between 0.01 M and 10 M. The rate of transformation increased as the OH^- concentration increased to 2 M and then remained constant. At lower OH^- concentrations, Mn_3O_4 transformed to a mixture of the 7-Å phase and γ-MnOOH, and at pHs of 7–9, it transformed to γ-MnOOH only (cf. Giovanoli *et al.*, 1976).

Very slow conversion into the 7-Å phase took place at 25°C. Increasing the temperature to 70° or 90°C markedly accelerated the reaction.

Progress of the transformation

The progress of the transformation with time is shown by a series of densitometer traces in Figure 2. After about 4% transformation, diffuse XRD lines arising from the 7-Å phase appeared at 7.09 and 3.53 Å (Figure 2b). These reflections became more intense as the reaction continued, and at the same time the reflections due to Mn_3O_4 gradually weakened. As the proportion of 7-Å phase in the system increased, a weak reflection at 7.67 Å appeared and a number of prism and pyramidal reflections could be seen (Figures 2c and 2d). At no stage during the transformation was there any evidence for $Mn(OH)_2$ as an intermediate phase.

TEM indicated that birnessite precipitated as very thin (<100 Å), irregular plates or films 2000–5000 Å across (Figures 3a and 3b). This initial precipitate recrystallized with time. Recrystallization was accompanied by an increase in the thickness of the films in the *c* direction (to several hundred Å), which led to some sharpening of the basal reflections in the XRD pattern. In the later stages of the transformation the product exhibited a mixture of morphologies, including irregular, thin plates, clumps or aggregates of films, and thicker, more structured plates or laths (Figures 3c and 3d). A similar mixture of morphologies as well as twinned crystals were present after 100% transformation (Figure 3e).

Recrystallization of birnessite in 1 M KOH at 70°C was slow and erratic. TEM indicated that recrystallization was far from complete several months after all the Mn_3O_4 had disappeared from the system. The rate-limiting step appeared to be the dissolution of birnessite. Increasing the OH^- concentration to 2 M and/or increasing the transformation temperature to 90°C markedly accelerated recrystallization.

Reaction products

Mn_3O_4-NaOH system. The XRD pattern of the transformation product of Mn_3O_4 in NaOH corresponded

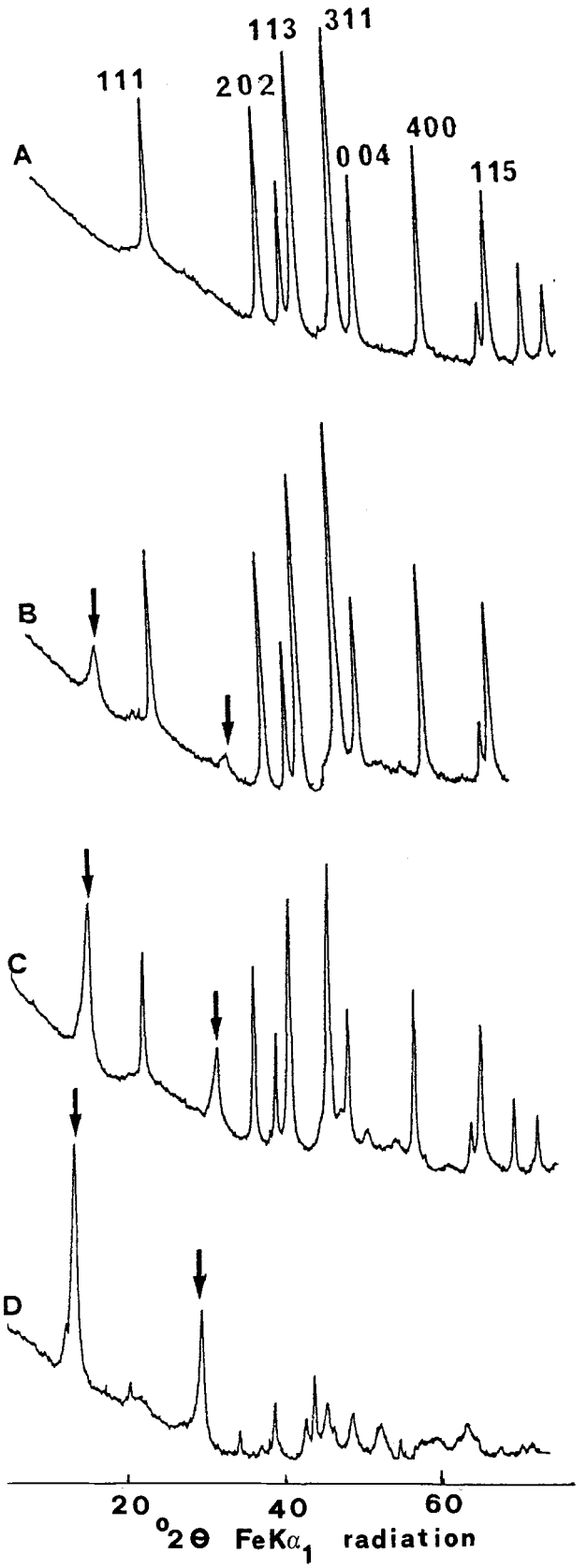

Figure 2. Densitometer curves of FeKα_1 Guinier-X-ray powder diffraction patterns showing extent of conversion of Mn_3O_4 into a 7-Å phase with time. Basal reflections of the 7-Å phase are arrowed.

https://doi.org/10.1346/CCMN.1988.0360306 Published online by Cambridge University Press

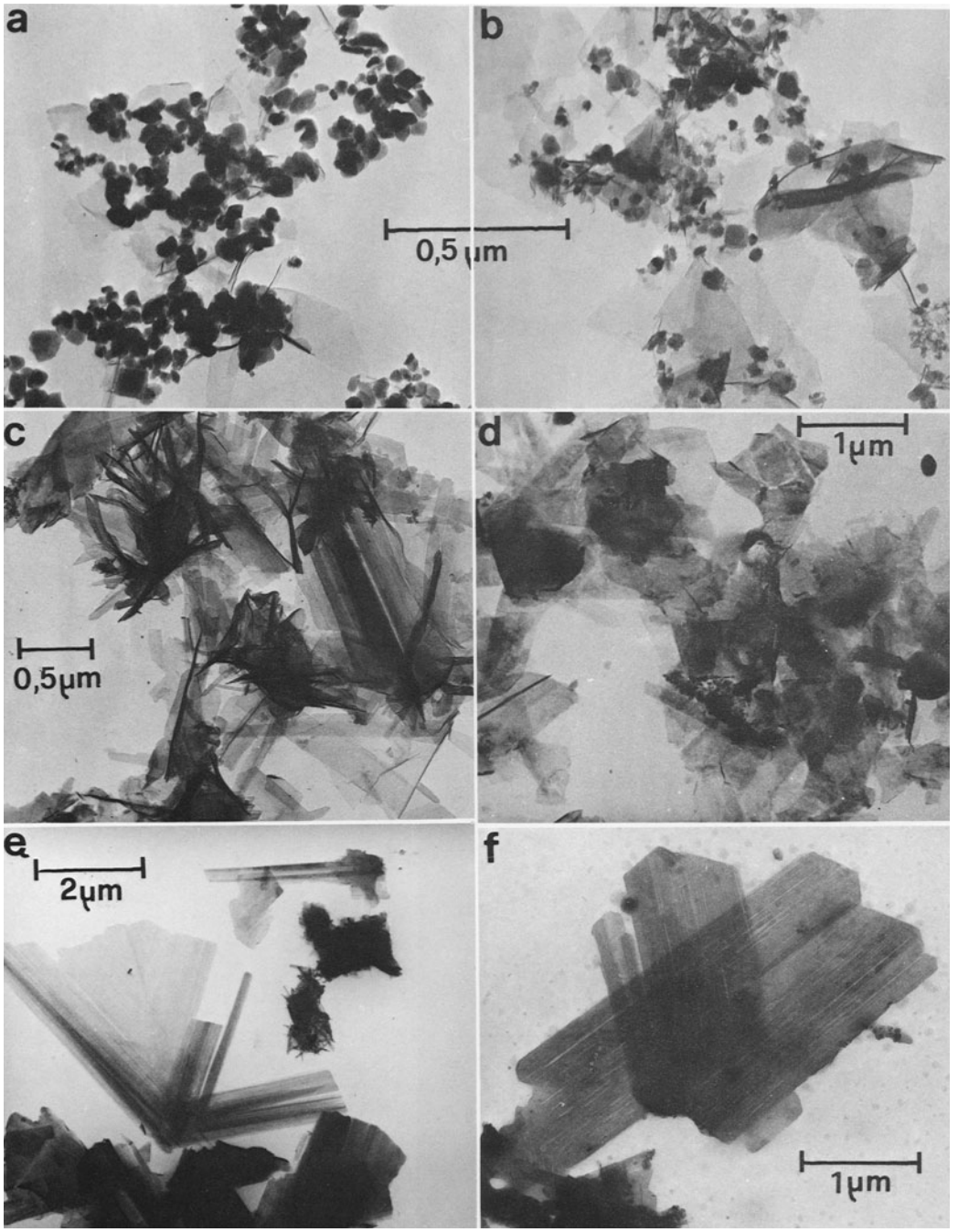

Figure 3. Transmission electron micrographs of the products of transformation of Mn_3O_4 in 1 M KOH, 70°C. (a) 4% conversion, mixture of Mn_3O_4 cubes and thin plates of the 7-Å phase; (b) 33% conversion; (c) 60% conversion, thin plates, masses of films, and some recrystallized laths; (d) 80% conversion; (e) recrystallized, twinned crystal of K-birnessite, 100% conversion; (f) recrystallized Na-birnessite twinned at 60° and displaying terminal 11.0 planes.

to that of $Na_4Mn_{14}O_{27}\cdot 9H_2O$ (Figure 4a). This material, which is a Na-birnessite having a basal spacing of 7.13 Å, was characterized by Giovanoli *et al.* (1970).

The Na-birnessite that formed by topotactic oxidation of $Mn(OH)_2$ had the same crystal size and shape (hexagonal platelets) as the parent material (Giovanoli *et al.*, 1970). The material that arose as a result of dissolution of Mn_3O_4, however, precipitated as thin plates and films. This initial precipitate did not represent an equilibrium morphology and gradually recrystallized in the mother liquor to thicker plates and laths which commonly terminated in well-developed

https://doi.org/10.1346/CCMN.1988.0360306 Published online by Cambridge University Press

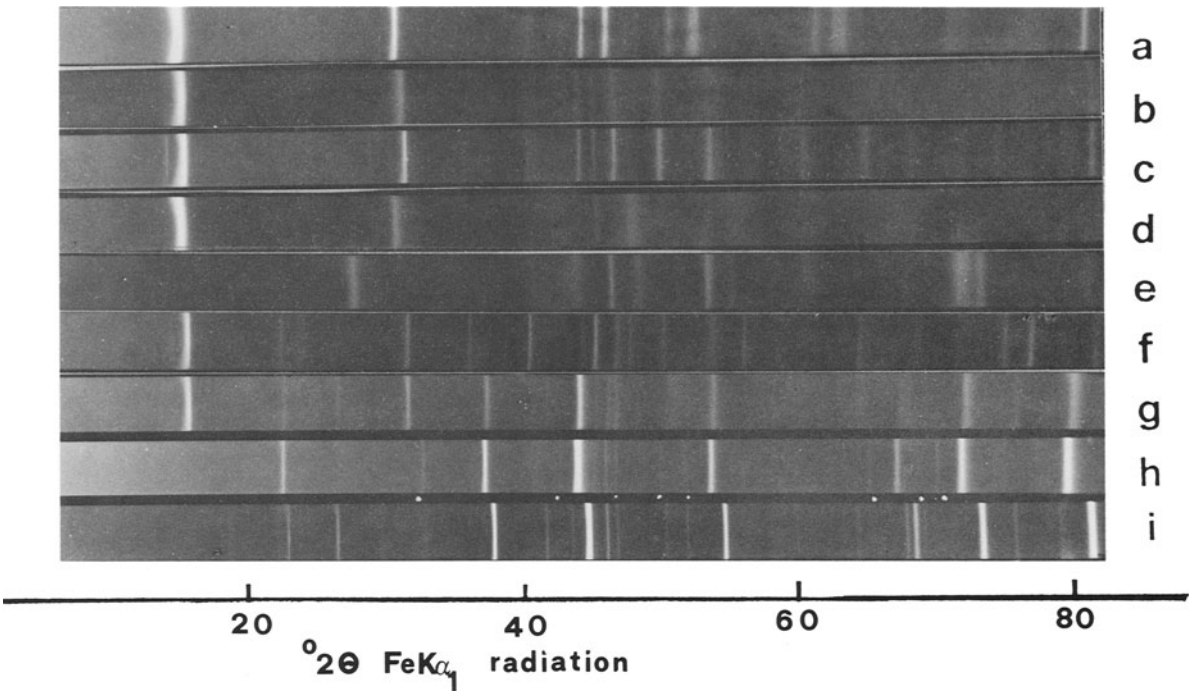

Figure 4. X-ray powder diffraction patterns of products of transformations carried out under a variety of conditions. (a) Na-birnessite ($Na_4Mn_{14}O_{27}\cdot 9H_2O$) formed from Mn_3O_4 in NaOH. (b) K-birnessite formed from Mn_3O_4 in KOH. (c) K-birnessite formed by holding the product formed in (a) in KOH. (d) $Mn_7O_{13}\cdot 5H_2O$ obtained by holding K-birnessite in water. (e) γ-MnO_2 obtained by holding K-birnessite in 0.1 M HNO_3. (f) Mn_3O_4 and K-birnessite formed from manganese(III) acetate in KOH. (g) Mixture of jacobsite, K-birnessite, and goethite (from jacobsite held in KOH for 5 months). (h) Mixture of jacobsite, γ-MnOOH, and trace of goethite (from jacobsite held at pH 8 for 5 months). (j) Mixture of Fe_3O_4 and goethite (from Fe_3O_4 held 3 months in KOH).

10.0 planes (Figure 3f). Much slower (years) recrystallization in water has been reported for a Na-bearing 10-Å phyllomanganate formed by oxidation of $Mn(OH)_2$ (Giovanoli, 1986).

Mn_3O_4-KOH system. The K-birnessite precipitated initially as very thin platelets (as much as 6000 Å across) which recrystallized to large, lath-like crystals having irregular ends (Figures 3a and 3e). These crystals were commonly twinned at 60°. The EDX spectrum of this birnessite showed peaks due to K (Figure 5), and chemical analysis gave a K:Mn ratio between 0.09 and 0.11.

The SAD pattern of this compound was hexagonal with $a_0 = 2.87$ Å (Figure 6). The diffraction spots were sharp and no streaking was present in the reciprocal lattice. The XRD pattern could not be indexed using a hexagonal unit cell. The true symmetry must, therefore, be orthorhombic or lower. For simplicity a pseudo-hexagonal cell can be given with $a_0 = 2.87$ Å and $c_0 = 7.09$ Å. Further work to determine the unit cell is in progress.

The XRD pattern of K-birnessite is shown in Figure 4b. The marked asymmetric broadening of the basal reflections is an indication of some disorder in the stacking of the $Mn(IV)O_6$ sheets along the *c* direction; locally wider spaces exist between the sheets. Comparison with the XRD pattern of Na-birnessite indicates that the two birnessites have different basal spacings and different numbers and positions of the prism and pyramidal reflections. In addition, K-birnessite has a characteristic weak reflection at 7.67 Å.

The basal reflections are more diffuse for K-birnessite than for Na-birnessite (Figures 4a and 4b), suggesting that even after recrystallization, the crystals of the former material were much thinner in the *c* direc-

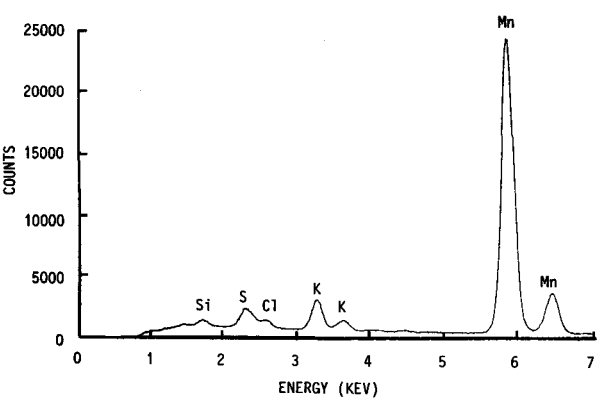

Figure 5. Energy dispersive X-ray spectrum of K-birnessite showing presence of K.

https://doi.org/10.1346/CCMN.1988.0360306 Published online by Cambridge University Press

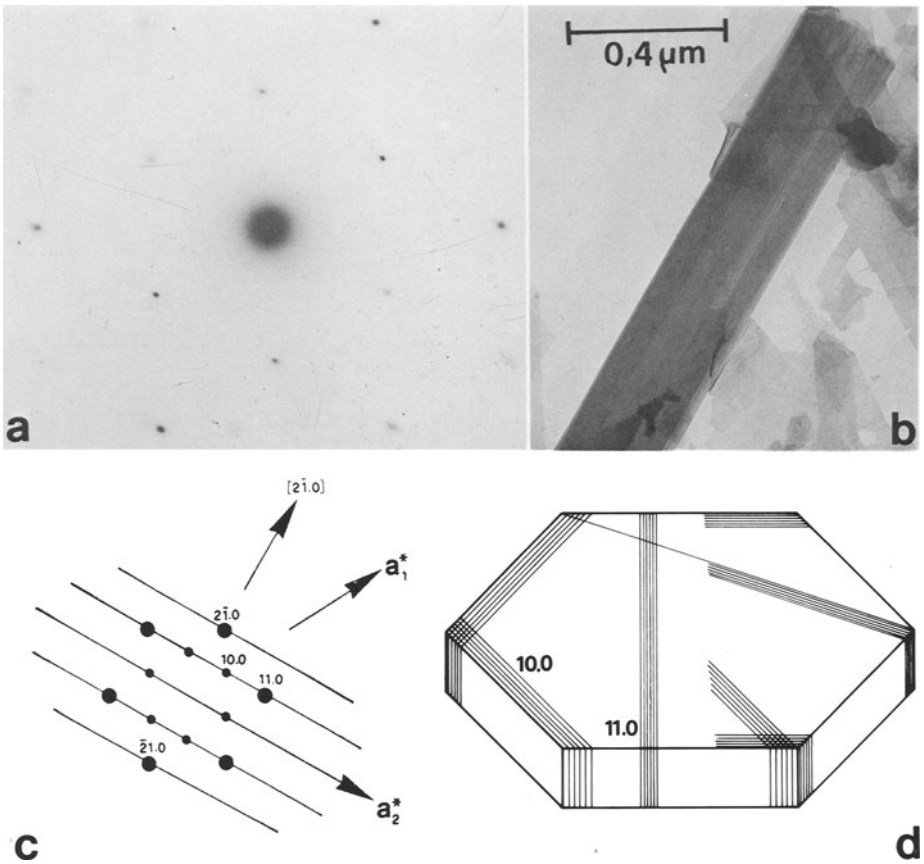

Figure 6. (a) Selected area electron diffraction (SAD) pattern of the crystal in (b) showing hexagonal diffraction patterns; (b) transmission electron micrograph of recrystallized lath of K-birnessite; (c) indexed SAD pattern; (d) schematic representation of crystal of K-birnessite; 10.0 and 11.0 planes are shown.

tion. The recrystallized Na-birnessite had a much lower surface area (8 m^2/g) than its K analogue (22 m^2/g), which can be attributed to differences in the average thickness of the crystals of the two compounds.

Interconversions between the birnessites. XRD showed that Na-birnessite could be converted completely into K-birnessite by treating it with 1 M KOH at 70°C for several days (Figure 4c). The EDX spectrum of the original Na-bearing material showed a peak due to Na, whereas for the final product, no such peak was noted and K peaks were observed instead. Chemical analysis confirmed that all the Na in the original 7-Å phase had been replaced by K.

Replacement of Na^+ by K^+ in Na-birnessite is a satisfactory route to a comparatively well-crystallized K-birnessite. TEM showed that exchange of cations was not accompanied by a change of crystal morphology. The XRD lines of the end product were, however, much sharper than those of the material formed directly by transformation of Mn_3O_4 in KOH (Figures 4b and 4c), reflecting the greater thickness of the crystals of the parent material.

In acid media complete replacement of Na^+ by K^+ or by transition metal ions has only been achieved for the Na-bearing 10-Å phyllomanganate. Uptake of transition metals by the Na-bearing 7-Å phase was slow and incomplete (Giovanoli and Brütsch, 1978). Most probably, complete exchange requires the more drastic conditions of high pH and 70°C used in the present work.

K-birnessite was resistant to Na exchange; it did not transform to Na-birnessite even after suspension in 1 M KOH at 70°C for three months.

Stability of K-birnessite. In view of the high level of K^+ in the system, the 7-Å phase should eventually have transformed to cryptomelane ($K_2Mn_8O_{16}$). TEM and XRD evidence, however, indicates that K-birnessite was stable in 1 M KOH and at 70°C for at least 12 months. Similarly, cryptomelane did not form from the 7-Å phase in 10 M KOH nor in KOH systems seeded with cryptomelane.

In neutral and acid media, K-birnessite readily transformed to other phases. After being held in twice-distilled water at 90°C for one week, the crystals were morphologically unchanged, but XRD measurements showed that the basal spacing had expanded from 7.09

https://doi.org/10.1346/CCMN.1988.0360306 Published online by Cambridge University Press

to 7.27 Å (Figure 4d). The XRD pattern of this material was identical to that of $Mn_7O_{13}\cdot 5H_2O$ (Giovanoli *et al.*, 1970) indicating that during the treatment in water, interlayer K^+ had been leached out and replaced by H^+. A similar transformation has been observed for Na-birnessite (Giovanoli *et al.*, 1970).

Under more acidic conditions (0.1 M HNO_3) the transformation proceeded further. The 7-Å phase dissolved and reprecipitated as poorly crystallized γ-MnO_2 (Figure 4e). With longer reaction times the transformation would probably have proceeded even further to give β-MnO_2 (cf. Giovanoli *et al.*, 1976). Buser *et al.* (1954) showed that in order for cryptomelane to form under these conditions a minimum K:Mn level in the system is necessary. In the present work, the K-birnessite was induced to transform to well-crystallized cryptomelane by holding it in a 0.1 M HNO_3 + 1 M KNO_3 solution for a few days at 70°C.

Formation of K-birnessite from an Mn^{3+} source. A 50:50 mixture of K-birnessite and hausmannite precipitated within 24 hr (70°C) from a solution of manganese(III) acetate in 1 M KOH (Figure 4f). All the prism, pyramidal, and basal reflections were present in the XRD pattern of the initial 7-Å phase precipitate. TEM showed that the 7-Å phase precipitated as a mixture of well-developed plates and laths, which appeared to be better formed than the initial precipitate obtained from dissolution of Mn_3O_4. This 7-Å phase was also far better defined morphologically than the clumps of thin films obtained by reduction of $KMnO_4$ in alkali (cf. Figure 9 in Giovanoli *et al.*, 1970). The hausmannite in the initial product transformed to K-birnessite within a few weeks at 90°C.

The present observation that precipitation of a 7-Å phase from a soluble Mn species is rapid is in agreement with earlier studies involving reduction of $KMnO_4$ (Giovanoli *et al.*, 1970). It also provides evidence that dissolution of Mn_3O_4 rather than nucleation of the 7-Å phase is the rate-limiting step in the Mn_3O_4 dissolution-reprecipitation transformation.

Transformation of other spinel phases in KOH

In 1 M KOH and at 70°C, jacobsite ($MnFe_2O_4$) was converted very slowly to a mixture of K-birnessite and goethite (α-FeOOH) (Figures 4g and 7a). In 1 M NaOH the corresponding Na-birnessite formed. Although the surface areas of jacobsite and hausmannite were comparable (22 m^2/g and 29 m^2/g, respectively), the transformation of jacobsite was much slower than that of hausmannite, and even after 5 months it was incomplete.

Some Mn released by dissolution of jacobsite was probably incorporated into the goethite structure. The crystals of goethite were long and thin (Figure 7a), typical of Mn-substituted goethite (Cornell and Giovanoli, 1987). The bulk of the Mn and Fe released, however, appeared to have precipitated as separate phases. No direct evidence was found that Fe was associated with birnessite, but the plates of this material were commonly thinner than those grown in an Fe-free environment, suggesting that growth in the *c* direction had been restricted to a greater degree than usual.

Further experiments into the effect of Fe on the transformation showed that in the presence of ferrihydrite, Mn_3O_4 was converted to very thin plates of birnessite (and goethite). These results are in line with Giovanoli's (1980) findings that in a Mn-Fe system, birnessite and iron oxides nucleate and grow independently of each other if the source of Mn is a separate solid phase. Neither ferrihydrite nor soluble Fe species (released by dissolution of jacobsite) prevented nucleation of birnessite. In Mn-Fe systems, this phase is suppressed only if Mn^{2+} and Fe^{3+} are coprecipitated to give Mn-ferrihydrite; this material transforms to Mn-goethite and jacobsite (Cornell and Giovanoli, 1987). Presumably, the end products depend on the rates of the various competing reactions involved as ferrihydrite dissolves. In water, jacobsite transformed, in an analogous manner to Mn_3O_4, into γ-MnOOH and a trace of goethite (Figure 4h).

Fe_3O_4 transformed in KOH to a mixture of twinned and acicular crystals of goethite (Figures 4i and 7b). No evidence was found for any intermediate ferrihydrite. Dissolution of Fe_3O_4 was extremely slow, hence the release of Fe was slow enough for the solubility product of goethite, but not ferrihydrite, to be exceeded. Twinned goethites usually nucleate in the ferrihydrite (Cornell and Giovanoli, 1985), but in this system, the twins apparently nucleated in solution. The twins were of the dendritic type that is thought to form in solution by a secondary nucleation mechanism if the growth of the parent crystal is disturbed (Maeda and Hirono, 1981). In this system, a possible disrupting species may have been Fe^{2+} released from Fe_3O_4.

DISCUSSION

The transformation of Mn_3O_4 to Na-birnessite in NaOH can be summarized by the following equation:

$$\frac{14}{3}Mn_3O_4 + 3.164\,O_2 + 4\,Na^+ + 4\,OH^- + 7\,H_2O \rightarrow Na_4Mn_{14}O_{27}\cdot 9H_2O.$$

The exact stoichiometry of the K-birnessite has not been determined, but a similar equation should describe the corresponding reaction in KOH.

The first step in the transformation is the dissolution of Mn_3O_4, followed by oxidation and disproportionation of the soluble dissolution products. The 7-Å phase forms by direct precipitation in solution. No $Mn(OH)_2$ intermediate was detected by XRD. Furthermore, the morphology of the crystals was different from that of crystals formed by topotactic transformation of

https://doi.org/10.1346/CCMN.1988.0360306 Published online by Cambridge University Press

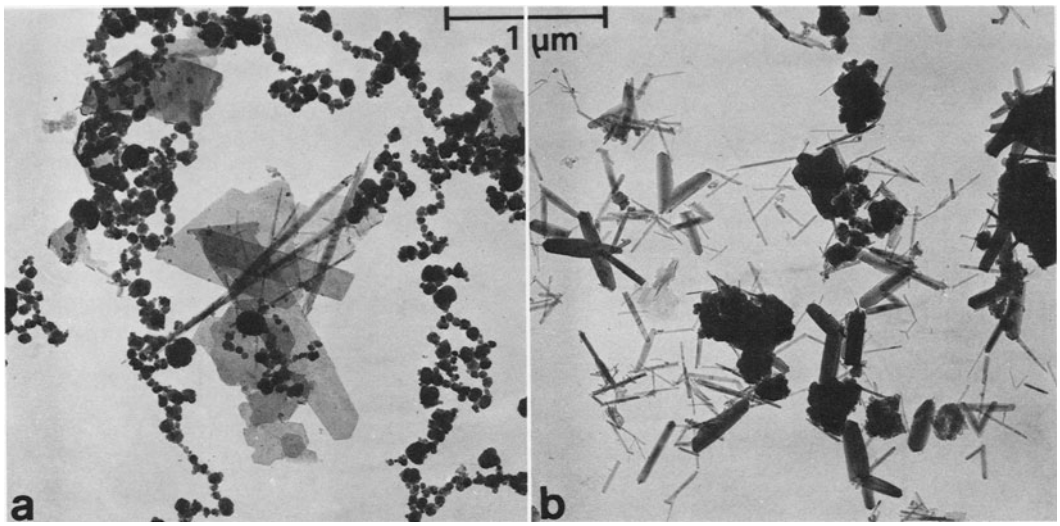

Figure 7. Transmission electron micrographs of (a) jacobsite and its transformation products in KOH; (b) twinned acicular crystals of goethite formed from Fe_3O_4 in 1 M KOH.

$Mn(OH)_2$. Although the initial induction period indicated that a certain degree of supersaturation was necessary for nucleation, formation of the 7-Å phase was rapid once the threshold level of soluble Mn species had been reached. The rate-limiting step in this transformation is the dissolution of Mn_3O_4.

This transformation, involving the dissolution of a spinel structure and reprecipitation of a layer structure is an extension of the interconversions between Mn_3O_4 and other Mn oxides (Figure 8). The similar behavior of Fe_3O_4 and $MnFe_2O_4$ suggests that dissolution in alkali followed by precipitation of a thermodynamically more stable phase may be characteristic of spinel structures.

Dissolution studies of spinels have usually been prompted by the need to remove scale produced in nuclear power stations. Attention has, therefore, been concentrated on reactions in acid media and in the presence of chelating agents. Bruyere and Blesa (1985) showed that Fe_3O_4 has an appreciable solubility in water at pH 12, but its dissolution behavior in alkali appears

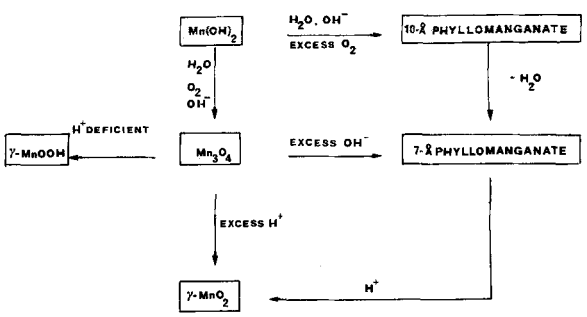

Figure 8. Schematic representation of interconversions between Mn_3O_4 and other Mn oxides.

to have been neglected. The oxides considered in the present work dissolved in alkali in the order (after correction for differences in surface area) Mn_3O_4 > $MnFe_2O_4$ > Fe_3O_4. The intermediate position of jacobsite in this series reflects the presence of both Mn and Fe in the structure, the rate of dissolution being governed by the slower rate of release of Fe from the structure (cf. Valverde, 1976).

Although Na-birnessite is the best characterized of the synthetic 7-Å phases, K-birnessite has also been reported in the literature (Golden *et al.*, 1986; Strobel and Charenton, 1987). K-birnessite was formed either by topotactic oxidation of $Mn(OH)_2$ in the presence of K^+ at high pH, or by K^+ exchange of the Na-birnessite produced by a topotactic transformation. The initial morphology of these compounds resembled that of the parent material, whereas the 7-Å phase formed by direct precipitation consisted of thin plates and films. The XRD patterns of both types of compounds differed only in the absence of the reflection at 7.67 Å in the patterns of the former 7-Å phases. This difference may, in fact, be an artefact. The 7.67-Å line is plainly visible in Guinier powder patterns, but not in diffractograms, and it is the latter that have been published in the literature. The reason for this difference between the two instruments is probably that the Guinier camera is more sensitive than the diffractometer.

K-birnessite represents a distinct member of the family of birnessites. It has a different unit cell from that of Na-birnessite and a smaller basal spacing of 7.09 Å compared with 7.13 Å for the Na form. The difference in the size of the hydrated cations appears to be responsible for the difference in the basal spacing of the two compounds. The interlayer cations are hydrated and, although K^+ has a larger ionic radius (1.13

Å) than Na^+ (0.95 Å), the reverse holds for hydrated cations. Na^+ has a hydrated radius of 2.76 Å, whereas the hydrated radius of K^+ is 2.32 Å (Fergusson, 1982).

In neutral or slightly acid media, both Na^+ and K^+ can be washed out of the 7-Å phase to give $Mn_7O_{13} \cdot 5H_2O$, an alkali, metal-free 7-Å phase. This result suggests that Na- and K-birnessites have the same basic structure. Their essential difference appears to be in the proportion and ordering of the alkali ions, with K^+ being less ordered.

K-birnessite is more stable against cation exchange than Na-birnessite. Similar stability has been reported for the K-vermiculites (van Olphen, 1977). In both types of compound the size of K^+ is such that it fits particularly well into the interlayer region and, hence, is difficult to displace.

K-birnessite appears to be the end member of the transformation series in KOH, at least at temperatures <100°C. This phase is sometimes found as an unwanted byproduct in discharged, alkaline Mn batteries. Laboratory studies have shown that this phase is also formed by the reduction of electrolytic γ-MnO_2 in 6 M KOH (Holton *et al.,* 1985). The reactions taking place have not been fully investigated, but reduction of γ-MnO_2 may lead to an intermediate Mn_3O_4 phase which then dissolves to give the K-bearing 7-Å phase.

ACKNOWLEDGMENTS

We are indebted to E. Ettinger for carrying out the electron microscopy and to M. Faller for the X-ray powder diffraction measurements. Thanks are due to B. Trusch for carrying out the BET measurements. Financial support by the Swiss National Foundation is acknowledged.

REFERENCES

Bruyere, V. I. E. and Blesa, M. A. (1985) Acidic and reductive dissolution of magnetite in aqueous sulphuric acid. Site-binding model of experimental results: *J. Electroanal. Chem. Interfacial Electrochem.* **182,** 141–156.

Buser, W., Graf, P., and Feitknecht, W. (1954) Beitrag zur Kenntnis der Mangan(II)manganite und des γ-MnO_2: *Helv. Chim. Acta* **37,** 2322–2333.

Cornell, R. M. and Giovanoli, R. (1985) Effect of solution conditions on the proportion and morphology of goethite formed from ferrihydrite: *Clays & Clay Minerals* **33,** 424–432.

Cornell, R. M. and Giovanoli, R. (1987) Effect of manganese on the transformation of ferrihydrite into goethite and jacobsite in alkaline media: *Clays & Clay Minerals* **35,** 11–20.

Cornell, R. M., Posner, A. M., and Quirk, J. P. (1975) The complete dissolution of goethite: *J. Appl. Chem. Biotechnol.* **25,** 701–706.

Fergusson, J. E. (1982) *Inorganic Chemistry and the Earth:* Pergamon Press, Oxford, 316 pp.

Giovanoli, R. (1976) Vom Hexaquo-Mangan zum Mangan-Sediment. Reaktionssequenzen feinteiliger fester Manganoxidhydroxide: *Chimia* **30,** 102–103.

Giovanoli, R. (1980) Layer structured manganese oxide hydroxides. VI. Recrystallization of synthetic buserite and the influence of amorphous silica and ferric hydroxide on its nucleation: *Chimia* **34,** 308–310.

Giovanoli, R. (1986) Manganese oxide minerals: in *Transactions XIII Congress Inter. Soc. Soil Sci., 1986, Vol. 5,* B. Hintze, ed., Int. Soc. Soil Science, Hamburg, 335–345.

Giovanoli, R. and Brütsch, R. (1978) L'Echange des ions de transition par le manganate-10Å et le manganate-7Å: in *La Genèse des Nodules de Manganèse,* Cl. Lalou, ed., Colloques Int. du CNRS, no. 289, Paris, 305–315.

Giovanoli, R., Feitknecht, W., Maurer, R., and Häni, H. (1976) Über die Reaktion von Mn_3O_4 mit Säuren: *Chimia* **30,** 307–309.

Giovanoli, R., Stähli, E., and Feitknecht, W. (1970) Über Oxidhydroxide des vierwerigen Mangans mit Schichtengitter. I. Natriummangan(II,III)manganate(IV): *Helv. Chim. Acta* **53,** 209–220.

Golden, D. C., Dixon, J. B., and Chen, C. C. (1986) Ion exchange thermal transformation and oxidizing properties of birnessite: *Clay & Clay Minerals* **34,** 511–520.

Hem, J. D. and Lind, C. J. (1983) Nonequilibrium models for predicting forms of precipitated manganese oxides: *Geochim. Cosmochim. Acta* **47,** 2037–2046.

Hixon, A. W. and Crowell, J. H. (1931) Dependence of reaction velocity upon surface agitation: *Ind. Eng. Chem.* **23,** 923–981.

Holton, D. M., Maskell, W. C., and Tye, F. L. (1985) The behaviour of γ-MnO_2 and reduced forms in concentrated potassium hydroxide solution: in *Power Sources 10,* L. Pearce, ed., Paul Press Ltd, London, 247 pp.

Maeda, Y. and Hirono, S. (1981) Electron microscopic observations on the dendrites of synthetic α-FeOOH particles: *Japan. J. Appl. Phys.* **20,** 1991–1992.

Strobel, P. and Charenton, J.-C. (1987) On the synthesis of various non-stoichiometric forms of manganese dioxide: *Rev. Chim. Miner.* **24,** 1–22.

Stumm, W. and Giovanoli, R. (1976) On the nature of particulate manganese in simulated lake waters: *Chimia* **30,** 423–425.

Valverde, N. (1976) Investigations on the rate of dissolution of ternary oxide systems in acidic solutions: *Ber. Bunsenges. Phys. Chem.* **81,** 380–384.

van Olphen, H. (1977) *Clay Colloid Chemistry,* 2nd ed., Wiley, New York, 318 pp.

(Received 14 July 1987; accepted 14 October 1987; Ms. 1689)